



Applications of Transitiometry: Determination of Thermophysical Properties and Decomposition Kinetics of Peroxide(Mixtures) Under High-Pressure

Svenja Albus¹ · Jonas Nowotny¹ · Jana Sartorius¹ · Markus Busch¹

Received: 8 December 2022 / Accepted: 19 February 2023 / Published online: 17 April 2023
© The Author(s) 2023

Abstract

Scanning transitiometry is an important calorimetric method co-invented by Jean-Pierre E. Grolier and Stanisław L. Randzio. Transitiometry enables to measure highly sensitive under high-pressure and high-temperature conditions. Nowadays, process modelling is a tool of increasing importance beyond the process of understanding process dynamics. For a valid modelling approach, a reliable data base at process conditions is required. Many processes are carried out at high temperature and pressure. Under such harsh conditions, comparatively few methods can be applied and thus limited kinetic parameters are known. Therefore, extrapolated values from low-pressure data are often utilized. Transitiometry can reduce this data gap for thermophysical properties such as heat capacity, thermal expansion coefficient and isothermal compressibility. In this paper, an overview about the method evaluation to determine thermophysical properties under high pressure using transitiometry is given. Additionally, an oversight is provided of the investigation of the decomposition kinetics of peroxides and their mixtures as another application area of high-pressure calorimetry.

Keywords High pressure · Kinetics · Peroxide decomposition · Thermophysical properties · Transitiometry

1 Introduction

In general, calorimetry deals with the measurement of the heat flux of samples. Chemical or physical processes and reactions can release or absorb heat and therefore be examined in a calorimeter. A widely and frequently applied calorimetric measuring principle is Differential Scanning Calorimetry (DSC) [1]. However, common DSC is often not adequate for special applications, such as measurements under high-temperature and high-pressure conditions. For calorimetric measurements up to a pressure of 700 MPa and temperatures up to 500 K, special equipment is needed. Scanning transitiometry represents a suitable

✉ Markus Busch
markus.busch@pre.tu-darmstadt.de

¹ Ernst-Berl-Institut für Technische und Makromolekulare Chemie, TU Darmstadt, Alarich-Weiss-Straße 8, 64287 Darmstadt, Germany

measurement method, for measurements under such harsh conditions. This technique was co-invented by Jean-Pierre E. Grolier and Stanisław L. Randzio. It allows the simultaneous regulation and determination of the three main thermodynamic variables temperature, pressure and volume during calorimetric measurement. This enables the investigation of a variety of thermophysical coefficients [2, 3].

A major advantage of scanning transitiometry is that not only liquids and their mixtures, but also gases and solid samples, for example polymers and their melts, can be analysed isobarically over large temperature and pressure ranges. Due to the simultaneous control of pressure, temperature and volume, transitiometry enables the application of more diverse experimental settings than a classic DSC. Moreover, the pressure range of up to 3000 bar and its isobaric mode exceeds the technical limitation of other calorimeters. Equally advantageous is the Tian–Calvet arrangement of the thermocouples and the detection of the heat signal in the transitiometer. In this set-up, the thermocouples are arranged three dimensionally around the sample, which largely eliminates the heat flow rate that is not detected by the sensor and up to 94% of the transferred heat can be detected. This improves greatly the accuracy of the measurements [4]. It was already revealed that thermophysical properties such as thermal expansion coefficient, α_p , and isobaric heat capacity, C_p , do not always behave as expected at high pressures [5, 6]. Besides the determination of thermophysical properties of various substances with scanning transitiometry [6–8], the technique ensures a better understanding of the effects of extrusion processing [9], for the determination of phase transitions and bubble point pressure in crude oils [10] or the investigation of decomposition kinetics of peroxides as well [11]. Apart from these multiple applications, transitiometry can also be utilized for the characterization of reactions or for the gathering of safety information.

2 Theoretical Background

Through the possible variation and control of pressure, volume and temperature during a measurement with scanning transitiometry, almost every differentially measurable transformation of state function can be determined. The heat flux difference as thermal output and the number of steps of the step motor as mechanical output is recorded and measured. The four different measurement options and modes of operation of transitiometers are shown in Table 1.

For the determination of thermophysical properties, mainly heat capacities, several measurement methods are already established in the literature. As not every method is suitable for every device, method evaluation is important. Nowotny [6] has performed a method of evaluation for the determination of thermophysical properties in scanning transitiometers and DSC. Different methods with various substances and sample holders were evaluated and compared in terms of their applicability in DSC and transitiometry, summarized in Table 2, as well as their reproducibility and accuracy of the results.

Nowotny [6] could prove that the pressure-step and pressure-scan methods are the most suitable applications for determination of heat capacities and expansion coefficients in transitiometers. Thereby, the pressure-scan method represents the fastest, most reproducible and accurate measurement method at high pressures when applied to pure liquids or gases. Methods which are based on a temperature program are not suited for the determination of heat capacities in the transitiometer. This is because of a lack of measurement speed and

Table 1 Four possible modes [5] of operation of a transitiometer are shown

Input		Thermal response	Mechanical response
$dT=0$ $p=f(t)$	$\rightarrow p, V, T$ —schedule \rightarrow	$\left(\frac{\partial S}{\partial p}\right)_T \rightarrow \alpha_p$	$\left(\frac{\partial V}{\partial p}\right)_T \rightarrow \kappa_T$
$dT=0$ $V=f(t)$	$\rightarrow p, V, T$ —schedule \rightarrow	$\left(\frac{\partial S}{\partial V}\right)_T \rightarrow \beta_V$	$\left(\frac{\partial V}{\partial p}\right)_T \rightarrow \kappa_T$
$dp=0$ $T=f(t)$	$\rightarrow p, V, T$ —schedule \rightarrow	$\left(\frac{\partial H}{\partial T}\right)_p \rightarrow c_p$	$\left(\frac{\partial V}{\partial T}\right)_p \rightarrow \alpha_p$
$dV=0$ $T=f(t)$	$\rightarrow p, V, T$ —schedule \rightarrow	$\left(\frac{\partial U}{\partial T}\right)_V \rightarrow c_v$	$\left(\frac{\partial p}{\partial T}\right)_V \rightarrow \beta_V$

One parameter (p , T or V) is kept constant, a second is varied by a predetermined program and a third is measured as a function of the other two. In addition to the three state variables mentioned, the change of enthalpy H , internal energy U and entropy S can also be recorded

Table 2 Methods for the determination of heat capacities in DSC and transitiometry with a recommendation of the best method for specific application

	DSC		Transitiometry	
	Aluminium	High-pressure	Cell type 1	Cell type 2
Three-step method	++	+	+	+
Two-step method	+	–	–	–
Temperature-step method	++	+	+	–
Pressure-scan method	--	–	++	++
Pressure-step method	--	–	++	++

In DSC aluminium crucibles and high-pressure crucibles were tested, in transitiometry two different types of cells. The two cells differentiate in their inlet volume in the area of detection and their possible pressure range. Cell type 1 are the thick-walled cells (up to 4000 bar) and cell type 2 are thin-walled cells (up to 1600 bar). The recommendation ranges from “++” for good method for this application, “+” for a possible application, “–” for a possible but restricted application and “--” for not possible with this set-up [6]

reproducibility due to the thick walls of the sample vessels and the change in the relative position of the vessels and the sensor.

To determine the pressure dependence of heat capacities (1) with the pressure-scan method, expansion coefficients and specific volume can be applied. Therefore, the expansion coefficient has to be evaluated from several isotherms over a pressure range. Obtaining an absolute heat capacity from the relative evaluated pressure-dependent capacity, a literature or simulated value of heat capacity at the lower pressure limit p_0 is required.

$$c_p = c_{p,0} - T \int_{p_0}^p v(p, T) \left[\alpha_p^2 + \left(\frac{\partial \alpha_p}{\partial T} \right)_p \right] dp. \quad (1)$$

Due to the explained preference for pressure scans rather than temperature scans, the expansion coefficients are evaluated from the isothermal heat flux φ following (3) [1] instead of from the isobaric mechanical output (2). Moreover, the pressure changing rate γ , the temperature T and the expansion coefficient of the cell $\alpha_{p,SS}$ are included. The calibration constant K reflects the contribution of the transitiometer and is obtained combining

the heat flux of a reference substance with well-known literature data of α . As reference substance, argon is applied for the advanced unit and toluene is used for the standard unit.

$$\alpha_p = \frac{1}{v} \left(\frac{\partial v}{\partial T} \right)_p, \quad (2)$$

$$\alpha_p = \alpha_{p,SS} - \frac{\varphi_S(p)}{\gamma T} \frac{K(p, T)}{V_E}. \quad (3)$$

Besides the expansion coefficient, the specific volume is evaluated from the mechanical output and is required to calculate the heat capacity. The mechanical output as number of steps each with a volume of $5.22 \times 10^{-6} \text{ cm}^3$ measures the volume change ΔV . Starting from an initial volume V and with known sample mass m , its density ρ , respectively, specific volume ν (Eq. 4) is obtained.

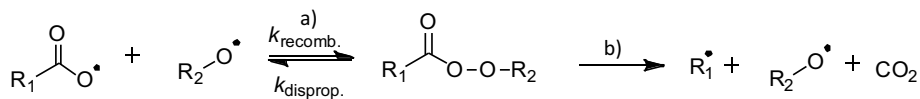
$$\rho = \frac{1}{\nu} = \frac{m}{V + \Delta V}. \quad (4)$$

Additionally, transitionmetry fits the investigation of peroxide decomposition due to its highly exothermal reaction and the application of peroxides and their mixtures as initiators in high-pressure fields, like radical (co)-polymerization processes.

The decomposition of peroxyesters (investigated in this work) can occur by rather than in two different mechanisms [12]: a one-bond scission and a concerted two-bond scission (Fig. 1).

Buback [12, 13] and Luft [14] have examined the decrease of peroxide concentration in an optical high-pressure viewing cell and thereby the kinetics of decomposition of pure peroxides. Sartorius [11] proved that scanning transitionmetry represents a suitable mechanism to determine decomposition kinetics of peroxides and possible influences of chemical environment thereon. The decomposition of di-tert-butyl peroxide (DTBP) in ethylbenzene at different pressures between 100 and 1000 bar were investigated and the kinetic parameters were determined. Well-corresponding data were found in literature. However, we are not yet aware of any literature data, investigating the decomposition kinetics of peroxide mixtures, although they are applied in many industrial processes.

Similarly, in the analysis of peroxide mixtures with scanning transitionmetry, the decomposition enthalpy from the scission of the oxygen–oxygen bonding is temporally recorded and utilized to calculate the reaction kinetics. The Borchardt and Daniels method constitutes, according to Sartorius [11], a suitable method for the determination of decomposition kinetics. Overlapping signals in peroxide mixtures, due to similar self-accelerating



TAPPI: $\text{R}_1=\text{C}_4\text{H}_9$; $\text{R}_2=\text{C}_5\text{H}_{11}$

TBPA: $\text{R}_1=\text{CH}_3$; $\text{R}_2=\text{C}_4\text{H}_9$

Fig. 1 Reaction mechanism of the decomposition of organic peroxyesters following **a** one-bond and **b** concerted double-bond scission, according to Buback [12]. The investigated peroxides tert-butyl peroxyacetate (TBPA) and tert-amyl peroxyvalate (TAPPI) belong to the group of organic peroxy esters, the specific residuals are indicated

decomposition temperatures (SADT), first need to be deconvoluted with OriginPro®. Thereafter, a regular evaluation with the Borchardt and Daniels method can be performed.

The Borchardt and Daniels method [15] connects calorimetric information about the time-dependent reaction enthalpy to the reaction progress α and the kinetics providing a determination of the pre-exponential factor A , the activation energy E_A and the order of reaction n from Eq. 5.

$$\ln\left(\frac{d\alpha}{dt}\right) = \ln(A) - \frac{E_A}{R \cdot T} + n \cdot \ln(1 - \alpha). \quad (5)$$

Activation volumes ΔV^\ddagger of the decomposition can be calculated according to Eq. 6 [12].

$$\left(\frac{\partial \ln k}{\partial p}\right)_T = -\frac{\Delta V^\ddagger}{RT}. \quad (6)$$

3 Experimental

3.1 Instrumentation

Measurements of thermophysical properties and decomposition kinetics of peroxides and their mixtures can be performed with scanning transitiometry. Thereby, a transitiometer standard unit from BGR TECH (SU) (Fig. 2) and a transitiometer advanced unit from BGR TECH (AU) are available.

Both the transitiometers possess two differentially connected, equal and independent measuring cells, a reference cell and a sample cell. While the sample can be placed in the measuring chamber (on a column of mercury in case of SU), the reference cell is filled with

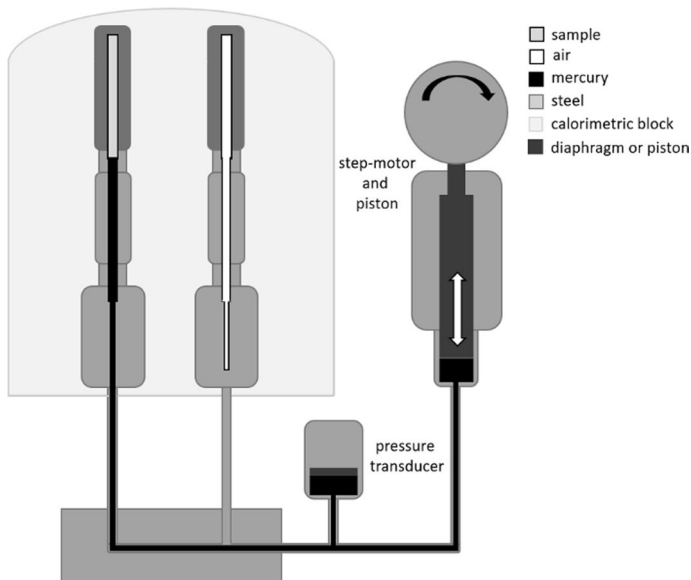


Fig. 2 Setup of the SU transitiometer from BGR TECH

air or an air-filled glass ampoule (in case of AU). The cells are made of Hastelloy C22 with a length of 25 cm and a diameter of 0.45 cm. The thermocouples are constructed cylindrically around the two cells according to the Tian–Calvet principle and cover the upper 8 cm, giving an approximate measurement volume of 1 mL. 1344 thermocouples are installed in the advanced unit and 672 thermocouples in the standard unit. The accuracies of the transitiometer measurements are very high because of the high number of thermocouples incorporated in the calorimetric block. The thermal resolution is up to 10^{-7} W according to the manufacturer, the temperature accuracy is given with $\pm 10^{-4}$ K and the pressure with $\pm 0.15\%$ full scale output. Due to the massive cells, only heating rates between 1 and $5 \text{ mK}\cdot\text{s}^{-1}$ can be realized.

To increase the pressure or to regulate it during the measurement, step motors are applied in both transitiometers, which can run an approximate volume of 9 cm^3 . One step of the motor in the AU corresponds to $5.24 \times 10^{-6} \text{ cm}^3$ and one in the SU of $5.22 \times 10^{-6} \text{ cm}^3$. In the SU, mercury is used as an almost incompressible medium to generate pressure, while gases are used in the AU. Both the mercury and the gases come into contact with the investigated substance.

Further detailed descriptions of the instruments are also given elsewhere [6, 16].

3.2 Materials and Sample Preparation

For the measurements of thermophysical properties, the cell is completely filled with the substance to be analysed. Therefore, liquids are directly placed in the SU on the mercury surface, molten polymers are separated from the mercury surface by a teflon spacer. Gases are investigated in the AU by pre-compressing them with a membrane compressor and a high-pressure syringe. The applied propylene is from Air Liquide and has a purity of $>99.5\%$. The polymer polypropylene (PP) used in this work has a molecular weight of $M_n = 22,600 \text{ g}\cdot\text{mol}^{-1}$ and $M_w = 151,000 \text{ g}\cdot\text{mol}^{-1}$.

The measurement set-up to determine thermophysical properties according to the pressure-step method is shown in Fig. 3. For the pressure-step method, 8000 s isobaric conditions are held to reach the thermophysical equilibrium before and after the pressure scan with a changing rate of $0.05 \text{ bar}\cdot\text{s}^{-1}$.

For the determination of decomposition kinetics of peroxides in the literature, predominantly heptane as solvent is applied. In this work, the investigation of the decomposition kinetics of peroxides and their mixtures is, in addition to heptane, performed in a higher

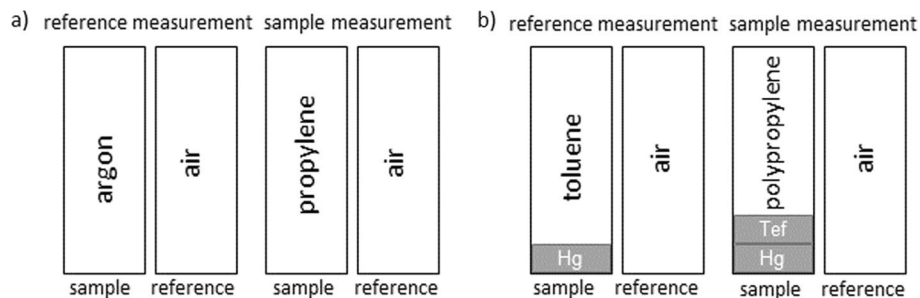


Fig. 3 Experimental set-up for applying the pressure-scan method in the **a** advanced unit and **b** standard unit. In the standard unit, the sample substances are placed directly on mercury (Hg) as pressurizing medium. Only the polymers are given on a teflon (Tef) spacer

viscous medium, squalane. This is to simulate a later stage in the polymerization process where the initiator molecule is surrounded by a matrix of monomer and polymer molecules. For a peroxide mixture, 10 wt% of each of the investigated peroxides TBPA and TAPPI are dissolved in squalane and stored in a freezer. For the investigation of pure peroxides, 10 wt% of TAPPI or TBPA is diluted in heptane or squalane and similarly refrigerated until required for use. During the measurement by means of scanning transitiometry, the prepared samples are placed directly on the mercury column and closed without air inclusion. All measurements for the determination of peroxide kinetics are performed under isobaric conditions with pressures up to 500 bar, 1000 bar or 2000 bar. A temperature program is selected, where the heating rate is $2 \text{ mK}\cdot\text{s}^{-1}$ and the temperature range between 300 and 450 K, depending on the occurrence of the decomposition signal of each peroxide. The peroxides TAPPI (75% in aliphates, United Initiators) and TBPA (50% in aliphates, United Initiators) were used as they were obtained, as well as *n*-heptane (>99%, Acros Organics) and squalane (96%, Sigma-Aldrich).

Examples of the raw kinetic data obtained from a decomposition measurement of 10 wt% TAPPI in squalane in the SU transitiometer are shown in Fig. 4.

4 Results and Discussion

4.1 Thermophysical Properties

Thermophysical data are the basis for describing properties of a substance and to map it with equations of state (EoS) and simulation. Due to scarce literature at high pressure, EoS are commonly fitted to experimental data at low or medium pressure and extrapolated to the high-pressure range. Thus, a comparison to literature validating a method like transitiometry is challenging [3, 5, 6, 11]. Compared to calorimetric parameters like the expansion

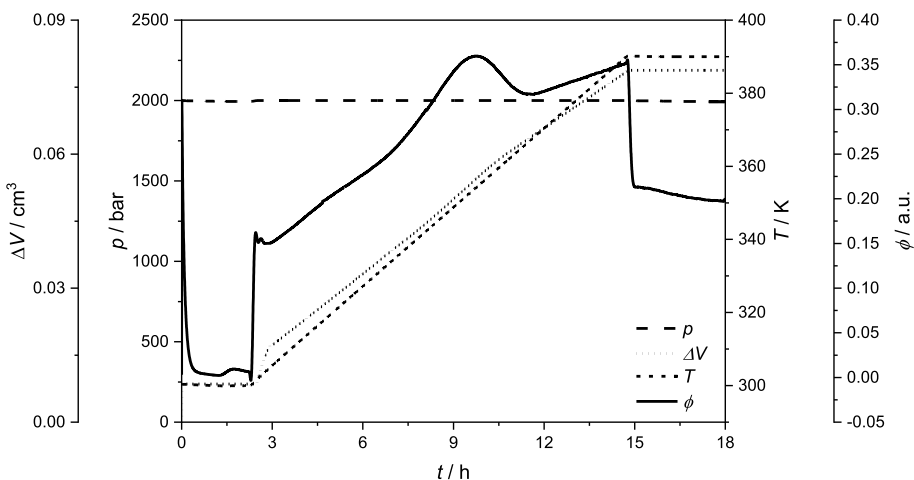


Fig. 4 Raw kinetic data of the decomposition of 10 wt% TAPPI in squalane. The measurement was performed at a constant pressure of 2000 bar during a temperature scan from 300 to 390 K with a heating rate of $2 \text{ mK}\cdot\text{s}^{-1}$. The heat flow ϕ and the volume ΔV covered by the stepping motor to ensure constant pressure over the entire measuring range are also recorded. A measurement point was recorded every 10 s

coefficient and heat capacity, volumetric data are broadly available and thus place density on a reliable data base and therefore, first chosen to validate the experimental results.

In this work, polypropylene and propylene are discussed as examples of polymer and gas samples, which are investigated with the standard unit transitiometer and advanced unit transitiometer. The density, the thermal expansion coefficient and the heat capacity are evaluated from several isothermal pressure scans. First, pressure- and temperature-dependent results for polypropylene are presented. In Fig. 5, the density of a polymer melt of polypropylene at 493 K measured by Nowotny [6] is compared to data found in literature.

As shown in Fig. 5, the densities of polypropylene show good agreement with literature data, despite different molecular weights of the polypropylene samples. The deviations of the measured data from Nowotny [6] and Zoller [17, 18] are within the precision tolerance from 5 to 6% of the measurements. The greater differences compared to Karl [20] and Forstner [19] may be explained by different molecular weights or experimental procedure. The density of polypropylene was measured by Nowotny [6] in a temperature range from 473 to 533 K and was furthermore fitted with Eq. 7. The calculated parameters are summarized in Table 3.

$$\rho(\text{g} \cdot \text{cm}^{-3}) = \frac{\rho_0 + A_{01}p + B_{01}T + B_{02}T^2 + B_{03}T^3}{1 + A_1p + A_2p^2 + A_3p^3 + B_1T + B_2T^2} \quad (7)$$

In summary, the standard unit transitiometer is suitable for measuring pressure- and temperature-dependent densities with high reproducibility and accuracy as well as in good agreement with the literature data [6]. Besides the mechanical output of the stepping motor for calculating pressure and temperature dependent density changes, the heat flux as thermal output during a pressure scan is recorded in transitiometers. This allows the evaluation of thermal expansion coefficients according to (3). Combined with the specific volume, heat capacities are calculated applying (1). Figure 6 shows the expansion coefficients and heat capacities of polypropylene measured by Nowotny [6] in the scanning transitiometer with the pressure-scan method in comparison with the literature data.

Nowotny [6] observed a phase transition from solid PP to liquid PP in the calculated expansion coefficients, shown in the blue layer in (a) when decreasing the pressure at 800 bar at the lowest isotherm of 473 K. Melting as a first-order phase transition

Fig. 5 Measured densities of polypropylene at 493 K in the standard unit transitiometer [6] compared to literature data [17–20]

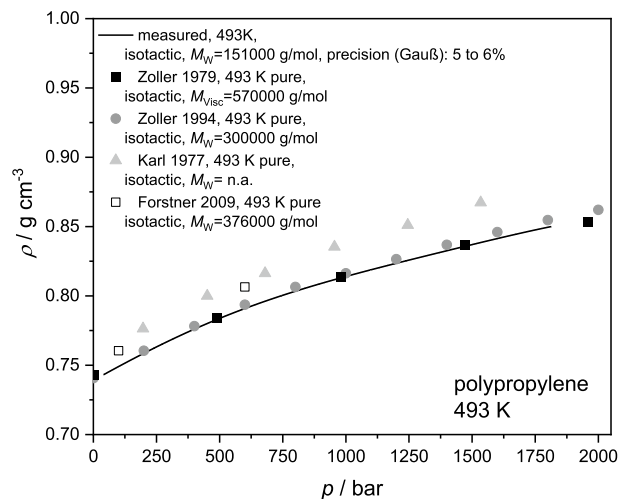


Table 3 Calculated parameters by fitting the experimental results of pressure- and temperature-dependent densities (7), expansion coefficients (8) and heat capacities (9) of PP, which were measured in the standard unit transiometer according to the pressure-scan method [6]

Pressure- and temperature-dependent densities of PP		Expansion coefficients of PP		Heat capacities of PP	
Parameter	Value	Parameter	Value	Parameter	Value
ρ_0	$-3.15\text{E}+00$	α_0	$-3.77\text{E}+02$	$c_{p,0}$	$-1.75\text{E}+03$
A_{01}	$-2.62\text{E}-04$	A_{01}	$-5.13\text{E}-02$	A_{01}	$-8.28\text{E}-03$
B_{01}	$3.04\text{E}-02$	B_{01}	$2.83\text{E}-01$	B_{01}	$1.93\text{E}+01$
B_{02}	$-6.37\text{E}-05$	B_{02}	$9.00\text{E}-04$	B_{02}	$-1.77\text{E}-02$
B_{03}	$3.96\text{E}-08$	B_{03}	$-5.84\text{E}-07$	B_{03}	$-3.83\text{E}-06$
A_1	$-5.61\text{E}-04$	A_1	$-8.50\text{E}+01$	A_1	$9.35\text{E}-05$
A_2	$1.18\text{E}-07$	A_2	$-2.65\text{E}-02$	A_2	$-3.57\text{E}-08$
A_3	$-2.21\text{E}-11$	A_3	$-2.37\text{E}-05$	A_3	$7.20\text{E}-13$
B_1	$5.74\text{E}-03$	B_1	$-1.95\text{E}+03$	B_1	$2.19\text{E}-03$
B_2	$-9.50\text{E}-06$	B_2	$3.41\text{E}+00$	B_2	$-4.23\text{E}-06$
R^2	0.9991	R^2	0.9891	R^2	0.9999
$T_{\text{range}}/\text{K}$	473 to 533	$T_{\text{range}}/\text{K}$	473 to 533	$T_{\text{range}}/\text{K}$	473 to 533
$p_{\text{range}}/\text{bar}$	40 to 2000	$p_{\text{range}}/\text{bar}$	20 to 2000	$p_{\text{range}}/\text{bar}$	20 to 2000

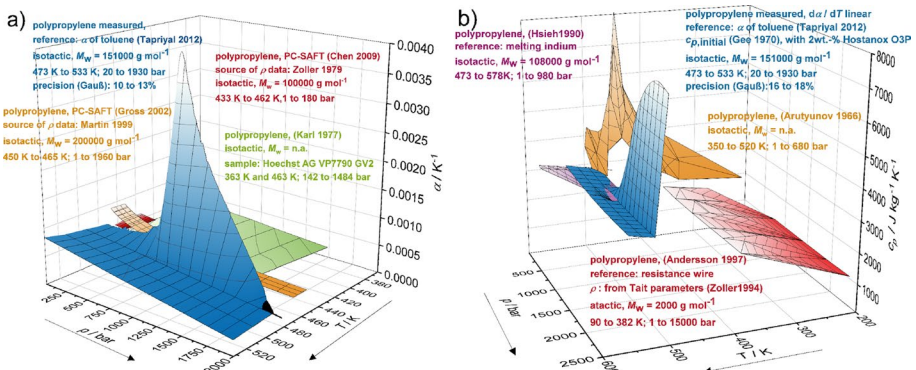


Fig. 6 **a** Measured expansion coefficients of polypropylene [6] in dependence of pressure and temperature which were measured with the pressure-scan method in the standard unit transiometer. For an evaluation of measured heat flux differences, expansion coefficients of toluene [21] calculated with perturbed chain statistical associating fluid theory (PC-SAFT) have been applied for polypropylene. The measured expansion coefficients are compared to the literature data [20, 22, 23]. **b** Measured heat capacities of polypropylene [6] in dependence of pressure and temperature which were measured with the pressure-scan method in the standard unit transiometer compared to experimentally determined literature data [24–26]

causes formally a skip function in the change of enthalpy and an infinite heat capacity, which is visible as a sharp peak. A comparison with the temperature- and pressure-extrapolated literature data [20, 22, 23] shows a concordance with the measured data at lower temperature. However, the expansion coefficients in the literature reveal a more linear pressure dependence than the measured data but cover a lower pressure range. In

the transitiometric pressure-scan measurements, the heat flux difference has the biggest impact on the calculation of the expansion coefficients. This is why an exact calibration of the devices and averaging of repeating measurements is very important to gain accurate results. The expansion coefficients of polypropylene were fitted by Nowotny [6] with pressure and temperature dependence (8), the coefficients are summarized in Table 3.

$$\alpha/(K^{-1}) = \frac{\alpha_0 + A_{01}P + B_{01}T + B_{02}T^2 + B_{03}T^3}{1 + A_{11}P + A_{21}P^2 + A_{31}P^3 + B_1T + B_2T^2}. \quad (8)$$

The calculated expansion coefficients are utilized to determine heat capacities according to Eq. 1. The experimentally determined heat capacities of polypropylene are compared to that given in the literature [24–26] in Fig. 6b. Nowotny [6] observed that above the melting point for the heat capacities of PP no literature data are available, but coincided with other to higher temperatures and pressures extrapolated experimental data. Additionally, the measured heat capacities decrease with pressure. Similarly, the measured heat capacities of polypropylene were fitted by Nowotny [6] with pressure and temperature dependence (9), the coefficients are summarized in Table 3.

$$c_p/(J \cdot kg^{-1} \cdot K^{-1}) = \frac{c_{p,0} + A_{01}P + B_{01}T + B_{02}T^2 + B_{03}T^3}{1 + A_{11}P + A_{21}P^2 + A_{31}P^3 + B_1T + B_2T^2}. \quad (9)$$

Table 3 summarizes the calculated parameters by fitting the experimental results of pressure- and temperature-dependent densities, expansion coefficients and heat capacities of PP from Eqs. 7 to 9 with the program OriginPro®.

The applicability of the pressure-scan method can be extended from liquids and polymers in the standard unit transitiometer to gases in the advanced unit transitiometer. In the following, propylene is presented as an example regarding the measurement of the thermal expansion coefficient and heat capacity. Due to the variation of mass during the pressure scan, no density can be determined. The remaining experimental procedure and evaluation is similar to the procedure applied to PP presented as an example for the standard unit transitiometer. Due to the gaseous nature of the sample, argon instead of toluene as reference substance is chosen because of its accurate predictable expansion coefficient. Using this to calculate the calibration constant using a PC-SAFT predicted thermal expansion coefficient and by AU measured heat flux, the expansion coefficient of propylene is evaluated (Fig. 7). Compared to PP, propylene exhibits a significantly higher expansion coefficient and a higher gradient at low pressure. Preventing possible formation of oligomers, the measurements are performed in the presence of a stabilizer which is placed outside the detection range of the thermocouples. Comparing stabilized and unstabilized experiments for low temperatures, the obtained heat flux indicates no disturbance due to its presence.

Incorporating the experimental thermal expansion coefficient and the specific volume estimated by PC-SAFT, the change of heat capacity is calculated depending on pressure and temperature. In Fig. 8, the non-linear behaviour of the heat capacity is obvious. This illustrates that for propylene as well as PP an extrapolation above the experimental range from medium pressure has to be considered critically.

Table 4 summarizes the calculated parameters by fitting the experimental results of expansion coefficients and heat capacities of propylene from Eqs. 8 and 9 with the program OriginPro®.

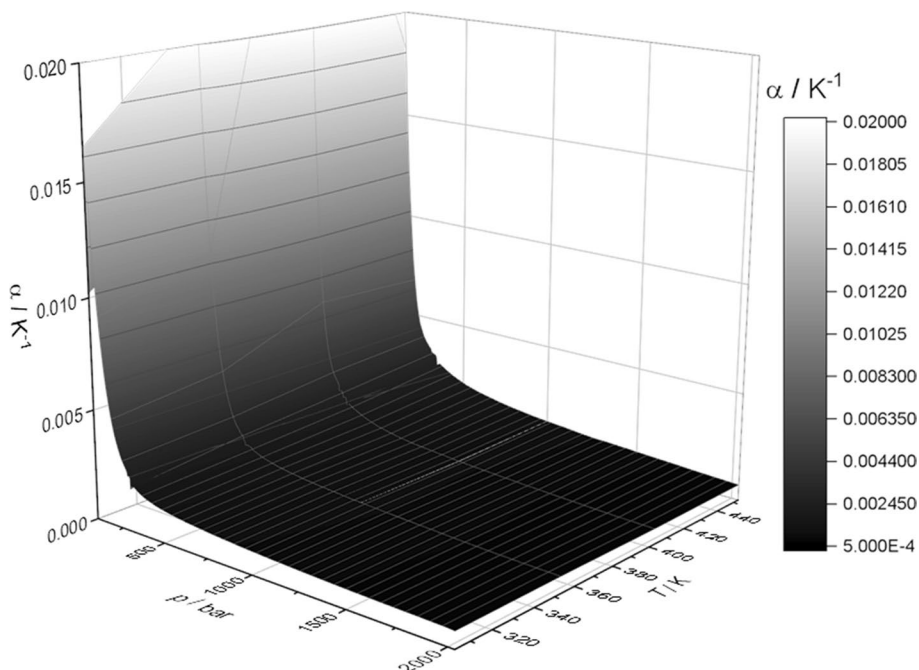


Fig. 7 Measured thermal expansion coefficient of propylene in the presence of 4-Methoxyphenol (MeHQ) as stabilizer in dependence of temperature and pressure evaluated from the pressure-scan method in the advanced unit transitiometer; argon is applied to calculate the calibration factor

4.2 Kinetic

Kinetic parameters of peroxide decomposition under high-pressure conditions are rarely presented in the literature. Buback [12, 13] and Luft [14] have investigated the decomposition kinetics of peroxides under elevated pressure conditions with isothermal IR spectroscopy. They monitored the absorption intensity of a vibration of a decomposition product, for example tertiary butanol. The results from Buback [12] are compared with own results from the calorimetric method in Fig. 9.

The reaction rate of the decomposition of TBPA in heptane decreases with pressure from 500 to 2000 bar, in the literature as well as our own data. With increasing the pressure the viscosity of the reaction environment around the sample also increases. Thereby, the mobility of the substances in the solvent is restricted, whereas the solvent cage is stabilized. This can lead to a more decelerated decomposition reaction as the diffusion of the decomposition products out of the cage is more restricted.

At higher temperatures, the experimental values drift further from the literature. This might be due to the difference in optical and calorimetric measurement methods. In the calorimeter, the heating rate is very slowly with $2 \text{ mK}\cdot\text{s}^{-1}$, so it is assumed that temperature and pressure are nearly constant for the entire measurement. In the experiments described in the literature, the solution needs a few seconds to reach a constant pressure and temperature, so that the heating time took up more of the residence time at higher temperatures and therefore the reaction tends to be slower. Furthermore, the decomposition products in the transitiometer are accumulated during the measuring period of

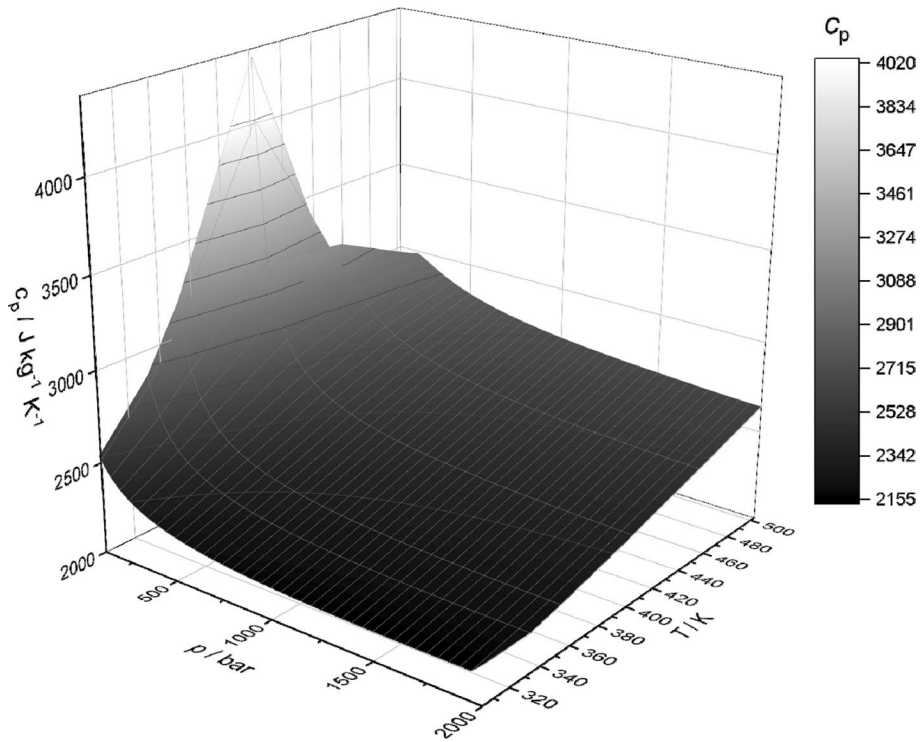


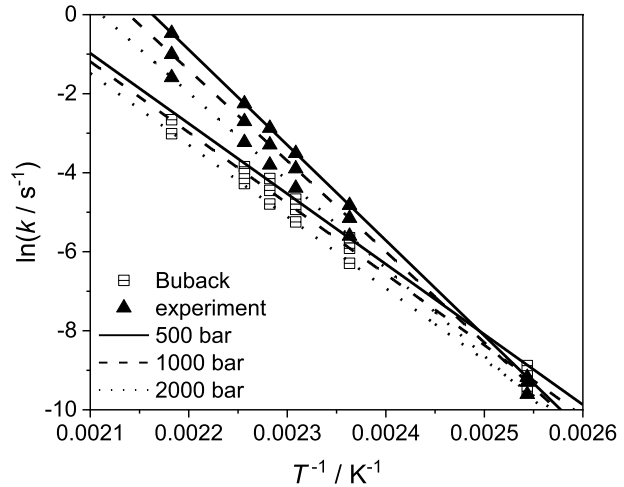
Fig. 8 Measured heat capacity of propylene in the presence of stabilizer MeHQ evaluated from the expansion coefficient and specific volume determined from PC-SAFT

Table 4 Calculated parameters by fitting the experimental results of expansion coefficients (8) and heat capacities (9) of propylene, which were measured in the advanced unit transiometer according to the pressure-scan method

Expansion coefficients of propylene		Heat capacities of propylene	
Parameter	Value	Parameter	Value
α_0	$-2.02\text{E}-03$	$c_{p,0}$	$3.42\text{E}+03$
A01	$7.89\text{E}-01$	A01	$8.44\text{E}-01$
B01	5.33	B01	$-2.29\text{E}+01$
B02	$1.50\text{E}+02$	B02	$4.25\text{E}-02$
B03	$-3.80\text{E}-05$	B03	$-1.24\text{E}-05$
A1	$-6.149\text{E}-01$	A1	$4.27\text{E}-04$
A2	0.35	A2	$-3.00\text{E}-08$
A3	$1.34\text{E}+03$	A3	$5.17\text{E}-12$
B1	$3.60\text{E}+01$	B1	-0.00621
B2	$-7.03\text{E}-02$	B2	$9.66742\text{E}-06$
R ²	0.7854	R ²	0.86167
$T_{\text{range}}/\text{K}$	303 to 453	$T_{\text{range}}/\text{K}$	303 to 503
$p_{\text{range}}/\text{bar}$	90 to 2000	$p_{\text{range}}/\text{bar}$	90 to 2000

several hours, whereas in the literature the entire decomposition occurs in a few seconds at one specific temperature.

Fig. 9 Temperature dependence of k for TBPA at 500 bar, 1000 bar and 2000 bar. Comparison between experimentally determined data with the literature data from Buback [12]



Subsequent experiments were performed in the higher viscosity medium, squalane, as solvent instead of *n*-heptane. The peroxide measurements in the literature were performed in heptane. This has technical reasons since more viscous media are not easy to handle. An advantage of transitiometry is that it can be applied to measure highly viscous media. Experimentally, it could be determined that by increasing the viscosity from *n*-heptane to squalane the decomposition reaction of TBPA was slowed down and the maximum decomposition peak temperatures were elevated.

Figure 10 displays the baseline corrected and mass normalized decomposition signals of TAPPI and TBPA and their mixture at 2000 bar in squalane.

The decomposition signals of TAPPI and TBPA in the mixture are broader than those of pure TAPPI and TBPA. During the decomposition of the peroxide mixture more heat is released which could indicate a modified decomposition mechanism. The maximum

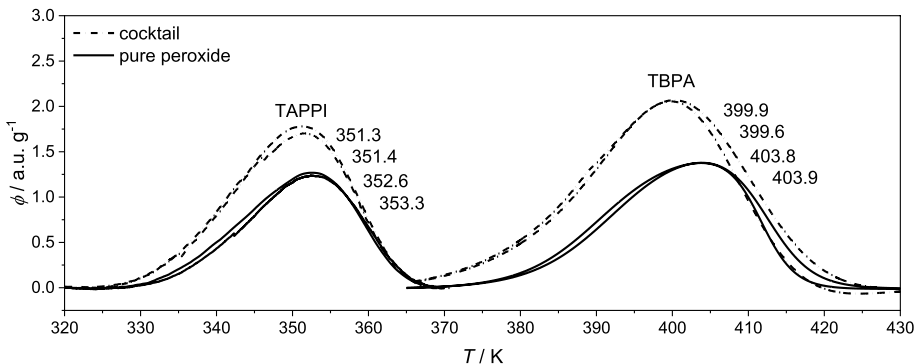
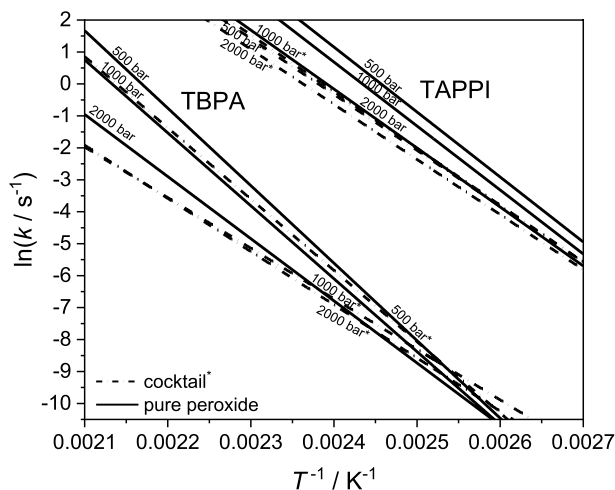


Fig. 10 Baseline corrected and mass normalized decomposition signals of 10 wt% of the individual peroxides TAPPI and TBPA (black solid line) and the mixture of both (black dashed line) in the solvent squalane, plotted against temperature. The measurements were performed twice each at the same conditions of 2000 bar. The maximum peak temperatures of the decomposition are shown next to the exothermic signals. The upper two show the maximum peak temperatures of the two measurements of the cocktail, the two below these of the individual peroxides

Table 5 Calculated kinetic parameters for the activation energy and the pre-exponential factor according to Borchardt and Daniels for the decomposition of peroxide mixtures of 10 wt% TAPPI and 10 wt% TBPA in comparison to the pure peroxides (10 wt%) at 2000 bar

	$E_A/kJ\cdot mol^{-1}$	A/s^{-1}
TBPA	154.28	2.12×10^{17}
TAPPI	148.45	1.46×10^{19}
Cocktail TBPA	132.00	2.26×10^{14}
Cocktail TAPPI	141.91	4.91×10^{17}

Fig. 11 Temperature dependence of k for a cocktail of 10 wt% TAPPI and 10 wt% TBPA (black dashed line) and 10 wt% TBPA (black dashed line) and 10 wt% of pure peroxides (black solid line) at 500 bar, 1000 bar and 2000 bar



decomposition temperatures of TAPPI and TBPA in the mixture are shifted to lower temperatures compared to that of the pure peroxides. The shift of the temperature maximum of the decomposition signal for TAPPI is in the range of 2 °C and 1.2 °C, which is less than the monitored shift for TBPA between 4.3 °C and 3.9 °C. During the decomposition of TBPA, the decomposition products of TAPPI are already present in solution. These might interfere with the decomposition mechanism of TBPA and therefore can influence it in some manner. However, by the decomposition reaction of TAPPI, since no or only few decomposition products are already existing, the maximum temperatures of the decomposition do not shift as significant. Not only the temperature but also the decomposition kinetics are influenced in the presence of another peroxides, as observed in Table 5.

Figure 11 shows the Arrhenius plots of the decomposition of a 10 wt% TAPPI and 10 wt% TBPA mixture and pure TAPPI and TBPA (each 10 wt%), measured at three different pressures.

The values for the reaction rate of the peroxide decomposition k belong to the cleavage of the oxygen–oxygen bond of the peroxide. Depending on the peroxide structure, the decomposition can preferably take place through mechanism (a) one-bond scission or (b) concerted two-bond scission (Fig. 1). k therefore describes the overall reaction rate of the decomposition, which is composed of these two steps. It was already observed by Buback [27] that the α -position of the carbonyl group of the peroxide plays an important role in which mechanism is preferred for decomposition.

The decomposition reaction of the peroxides TAPPI and TBPA in the mixture appears to be slower than that of the pure peroxides. This is illustrated by the Arrhenius plots of the peroxide cocktails, which are always below those of the pure peroxides for each pressure. Due to the presence of another peroxide in the solution, the decomposition reaction seems to be slowed down, possibly explained by interacting with further peroxides or decomposition products. Furthermore, the pressure dependency of the kinetics in this peroxide mixture appeared to be less strong. A crossing in the Arrhenius plots at lower temperatures of the peroxide cocktails with those of the pure peroxides at lower temperatures is observed, mainly for TBPA. This could be related to the fact that TBPA does not follow a first-order decomposition reaction. Broader decomposition signals may lead to slower decomposition and therefore a crossing of the Arrhenius plots.

The activation volumes, evaluated according to Eq. 6, of the decomposition reaction of TAPPI and TBPA in the mixture are lower than those of the pure peroxides at the same temperature range, as can be seen in Table 6. This fact coincides with the previous results that the kinetics of TAPPI and TBPA in a mixture featured lower kinetic parameters and maximum peak temperatures than TAPPI and TBPA alone. The activation volumes of the decomposition reaction of TBPA are higher than those of TAPPI at the same temperature ranges, which meets the results in literature taking different solvents into account.

5 Conclusion and Outlook

Experimental data at high-pressure conditions are crucial to improve EoS up to this range and better describe the behaviour of substances. More accurate process modelling ensures an adequate prediction and can be an efficient supplement to optimize the processes. The pressure-scan method is the most applicable one for the transistimeters to determine thermophysical properties and is validated among other substances by the comparison of PP to literature. Thus, density, thermal expansion coefficient and heat capacity are obtained in dependence of pressure and temperature and exceeding the documented ranges of other methods for polymers like PP, solvents and gases. As expected, the density increases with increasing pressure and decreasing temperature for PP. The thermal expansion coefficient decreases with rising pressure and temperature for PP and propylene. The heat capacity of both substances exhibits a more complex dependency on pressure and temperature. To utilize these properties for further calculations or modelling, their 3-D plot is fitted.

Comparative measurements of the decomposition kinetics of TBPA with literature data at different pressures revealed a good agreement between optical and calorimetric

Table 6 Experimental values for the activation volume for the decomposition of a cocktail containing 10 wt% TAPPI and 10 wt% TBPA in squalane and the pure peroxides determined according to Borchardt and Daniels method. The values for the activation volume were averaged over the temperature range

	T/K	p/bar	$\Delta V^\ddagger/\text{cm}^3\cdot\text{mol}^{-1}$
TBPA	393 to 458	500 to 2000	37.27
TAPPI	383 to 418	500 to 2000	24.88
Cocktail TBPA	393 to 458	500 to 2000	32.27
Cocktail TAPPI	383 to 418	500 to 2000	7.13

ΔV^\ddagger : activation volume

measurement method. The results of this work furthermore indicate that the decomposition kinetics of peroxide mixtures differ from those of the pure peroxides. Moreover, the maximum decomposition peak temperatures are shifted, peak shifts up to 4 °C could be observed for the peroxide mixture of TBPA and TAPPI. The results have provided a foundation for understanding the decomposition kinetics of peroxide mixtures at high-pressure conditions. However, it opens further fields to explore and can be the basis for future research. More peroxide mixtures should be investigated for a better understanding of their decomposition kinetics to find suitable peroxide concentration and composition of mixtures at reaction conditions with a view to design radical generation spectra over a wide temperature spectrum.

Acknowledgements The authors acknowledge United Initiators for supporting the kinetic investigation of organic peroxides.

Author contributions All authors contributed to the study conception and design, SA and JS wrote the main manuscript text. SA, JN and JS performed the experimental measurements and data analysis and were involved in investigation and methodology. MB contributed to project administration and supervision. All authors reviewed the manuscript.

Funding Open Access funding enabled and organized by Projekt DEAL. All authors contributed to the study conception and design. The authors did not receive support from any organization for the submitted work. No funding was received for conducting this study. The authors declare that they have no known competing financial interests that could have appeared to influence the work reported in this paper.

Declarations

Conflict of interest The authors have no relevant financial or non-financial interests to disclose. The authors have no competing interests to declare that are relevant to the content of this article. The authors have no financial or proprietary interests in any material discussed in this article.

Open Access This article is licensed under a Creative Commons Attribution 4.0 International License, which permits use, sharing, adaptation, distribution and reproduction in any medium or format, as long as you give appropriate credit to the original author(s) and the source, provide a link to the Creative Commons licence, and indicate if changes were made. The images or other third party material in this article are included in the article's Creative Commons licence, unless indicated otherwise in a credit line to the material. If material is not included in the article's Creative Commons licence and your intended use is not permitted by statutory regulation or exceeds the permitted use, you will need to obtain permission directly from the copyright holder. To view a copy of this licence, visit <http://creativecommons.org/licenses/by/4.0/>.

References

1. Höhne, G.W.H., Hemminger, W.F., Flammersheim, N.-J.: Differential Scanning Calorimetry. Springer, Berlin (2003)
2. Wilhelm, E.: In Memoriam: Jean-Pierre E. Grolier (1936–2022). *J. Solution Chem.* (2022). <https://doi.org/10.1007/s10953-022-01166-y>
3. Randzio, S.L.: Scanning transitionometry. *Chem. Soc. Rev.* (1996). <https://doi.org/10.1039/CS9962500383>
4. Schick, C.: Differential scanning calorimetry (DSC) of semicrystalline polymers. *Anal. Bioanal. Chem.* (2009). <https://doi.org/10.1007/s00216-009-3169-y>
5. Randzio, S.L.: State variables in calorimetric investigations: experimental results and their theoretical impact. *Thermochim. Acta* (1997). [https://doi.org/10.1016/S0040-6031\(97\)00032-4](https://doi.org/10.1016/S0040-6031(97)00032-4)
6. Nowotny, J.: Hochdruckkalorimetrie: methodenevaluierung und messung von wärmekapazitäten. In: *High-Pressure Calorimetry: Evaluation of Methods and Measurement of Heat Capacities* Darmstadt (2021)

7. Chorążewski, M., Grolier, J.-P.E., Randzio, S.L.: Isobaric thermal expansivities of toluene measured by scanning transitiometry at temperatures from (243 to 423) K and pressures up to 200 MPa. *J. Chem. Eng. Data* **55**, 5489 (2010). <https://doi.org/10.1021/je100657n>
8. Chorążewski, M., Dergal, F., Sawaya, T., Mokbel, I., Grolier, J.-P.E., Jose, J.: Thermophysical properties of normafluid (ISO 4113) over wide pressure and temperature ranges. *Fuel* **105**, 440–450 (2013)
9. Randzio, S.L., Orłowska, M.: Simultaneous and in situ analysis of thermal and volumetric properties of starch gelatinization over wide pressure and temperature ranges. *Biomacromolecules* (2005). <https://doi.org/10.1021/bm0503569>
10. Aquino-Olivos, M.A., Grolier, J.-P.E., Randzio, S.L., Aguirre-Gutiérrez, A.J., García-Sánchez, F.: Determination of the asphaltene precipitation envelope and bubble point pressure for a Mexican crude oil by scanning transitiometry. *Energy Fuels* **27**, 1212–1222 (2013)
11. Sartorius, J., Busch, M.: Kinetic investigation of peroxide decomposition by calorimetry under high-pressure. *Chem. Ing. Tech.* (2020). <https://doi.org/10.1002/cite.201900081>
12. Buback, M., Klingbeil, S., Sandmann, J., Sderra, M.B., Voegelé, H.P., Wackerbarth, H., Wittkowski, L.: Pressure and temperature dependence of the decomposition rate of tert-butyl peroxyacetate and of tert-butyl peroxyvalate. *Z. Phys. Chem.* **210**, 199–221 (1999)
13. Buback, M., Sandmann, J.: Pressure and temperature dependence of the decomposition rate of aliphatic tert-butyl peroxyesters. *Z. Phys. Chem.* (2000). <https://doi.org/10.1524/zpch.2000.214.5.583>
14. Luft, G., Mehrling, P., Seidl, H.: Decomposition of polymerization initiators under high pressures. *Angew. Makromol. Chem.* (1978). <https://doi.org/10.1002/apmc.1978.050730108>
15. Borchardt, H.J., Daniels, F.: The application of differential thermal analysis to the study of reaction kinetics. *J. Am. Chem. Soc.* (1957). <https://doi.org/10.1021/ja01558a009>
16. Randzio, S.L., Grolier, J.P.E., Chorazewski, M.: CHAPTER 14. High-pressure “Maxwell relations” measurements. In: Wilhelm, E., Letcher, T. (eds.) *Volume Properties: Liquids, Solutions and Vapours*, pp. 414–438. Royal Society of Chemistry, Cambridge (2014)
17. Zoller, P.: Pressure–volume–temperature relationships of solid and molten polypropylene and poly(butene-1). *J. Appl. Polym. Sci.* (1979). <https://doi.org/10.1002/app.1979.070230411>
18. Zoller, P., Fakhreddine, Y.A.: Pressure–volume–temperature studies of semi-crystalline polymers. *Thermochim. Acta* (1994). [https://doi.org/10.1016/S0040-6031\(94\)85221-9](https://doi.org/10.1016/S0040-6031(94)85221-9)
19. Forstner, R., Peters, G.W.M., Rendina, C., Housmans, J.W., Meijer, H.E.H.: Volumetric rheology of polymers. *J. Therm. Anal. Calorim.* (2009). <https://doi.org/10.1007/s10973-009-0552-z>
20. Karl, V.-H., Asmussen, F., Ueberreiter, K.: Über die druckabhängigkeit der viskoelastischen und physikalisch-chemischen eigenschaften von polymeren, 2. Spezifisches volumen und thermische ausdehnung einiger polymeren beim schmelzen und kristallisieren. *Makromol. Chem.* (1977). <https://doi.org/10.1002/macp.1977.021780718>
21. Tapriyal, D., Enick, R., McHugh, M., Gamwo, I., Morreale, B.: High Temperature, High Pressure Equation of State Density Correlations and Viscosity Correlations. National Energy Technology Laboratory, Morgantown (2012)
22. Chen, Z., Cao, K., Yao, Z., Huang, Z.: Modeling solubilities of subcritical and supercritical fluids in polymers with cubic and non-cubic equations of state. *J. Supercrit. Fluids* (2009). <https://doi.org/10.1016/j.supflu.2008.12.013>
23. Gross, J., Sadowski, G.: Modeling polymer systems using the perturbed-chain statistical associating fluid theory equation of state. *Ind. Eng. Chem. Res.* (2002). <https://doi.org/10.1021/ie010449g>
24. Hsieh, K.H., Wang, Y.Z.: Heat capacity of polypropylene composite at high pressure and temperature. *Polym. Eng. Sci.* (1990). <https://doi.org/10.1002/pen.760300808>
25. Andersson, S.P., Andersson, O.: Thermal conductivity, heat capacity, and compressibility of atactic poly(propylene) under high pressure. *Int. J. Thermophys.* (1997). <https://doi.org/10.1007/BF02575137>
26. Arutyunov, B.A., Bil, V.S.: Investigation of the thermophysical properties of polypropylene. *Mekh. Polim.* (1966). <https://doi.org/10.1007/BF00858717>
27. Buback, M., Nelke, D., Voegelé, H.-P.: Pressure and temperature dependence of the decomposition rate of aliphatic tert-amyl peroxyesters. *Z. Phys. Chem.* (2003). <https://doi.org/10.1524/zpch.217.9.1169.20402>